

FIG. 1. Effective collision frequency ν given by means of contours of constant $\nu v_d / \omega_{pe} v_{Te}$, and the electrostatic energy of the turbulence W given by means of contours of constant $W / nm_e v_{Te}^2$, expressed as a percentage.

It is difficult to compare the present theory with experimental results because the experimental parameters are time dependent and uncertain. However, if we consider the experiment of Hamberger *et al.*,⁵ the value of ν at the transition between the ion-sound and the two-stream instability is around $0.015\omega_{pe}$. Since this should occur at approximately $v_d = v_{Te}$, this corresponds to the $\nu v_d / \omega_{pe} v_{Te} = 0.015$ contour on the right-hand side of the first diagram in Fig. 1. We see then that there is at least rough agreement if the experimental value of T_i / T_e is not too large.

In conclusion we would say that the theory presented provides a simple description of ion-sound resistivity based on the physical processes which are known from numerical simulation to play the dominant role.

¹D. Biskamp and K. Chodura, *Phys. Rev. Lett.* **27**, 1553 (1971).

²A. Sykes and J. A. Wesson, in *Proceedings of the Fifth European Conference on Controlled Fusion and Plasma Physics, Grenoble, France, 1971*, (Service d'Ionique Generale, Association EURATOM-Commissariat à l'Energie Atomique, Centre d'Etudes Nucléaires de Grenoble, Grenoble, France, 1972), Vol. 1, p. 170.

³T. H. Dupree, *Phys. Fluids* **9**, 1773 (1966).

⁴J. Weinstock, *Phys. Fluids* **12**, 1045 (1969).

⁵S. M. Hamberger, J. Jancarik, L. E. Sharpe, D. A. Alderoff, and A. Wetherell, in *Proceedings of the Fourth International Conference on Plasma Physics and Controlled Nuclear Fusion Research, Madison, Wisconsin, 1971* (International Atomic Energy Agency, Vienna, 1972), Vol. 2, p. 37.

Heat Flow in the Extraordinary Phases of Liquid $^3\text{He}\dagger$

T. J. Greytak,* R. T. Johnson, D. N. Paulson, and J. C. Wheatley

Department of Physics, University of California at San Diego, La Jolla, California 92037

(Received 11 June 1973)

In a heat-flow experiment at zero field we have found that the phase diagram of liquid ^3He below the second-order transition at T_c divides into two regions. In one the heat flow is linear and enhanced by an amount predicted by a two-fluid model; the other shows non-linearity, history dependence, and critical-velocity effects. The two are separated by a line of thermal-resistance discontinuities which extrapolates to what may be a polycritical point at the line T_c and possibly to the "B" feature at the melting line.

At temperatures below 3 mK, liquid ^3He undergoes a second-order transition over a broad pressure range¹ to phases with extraordinary properties as shown by experiments both on²⁻⁴ and

off^{5,6} the melting curve. The present measurements are analogous to those of Brewer and Edwards^{7,8} on heat flow in capillary tubes containing superfluid ^4He , in which heat flows both diffusive-

ly and hydrodynamically. Hydrodynamic heat flow^{9,10} results from the viscous flow of normal fluid under the action of the fountain-pressure difference resulting from a temperature difference. A counterflow of superfluid adjusts itself to assure no net mass flow. The existence of hydrodynamic heat flow rests on the validity of the two-fluid model, and its measurement can lead to a determination of the normal fluid viscosity.

We have found in experiments in zero magnetic field that for pressures less than 21.5 bar the thermal resistance of a column of ³He decreases essentially discontinuously as the temperature decreases through the second-order transition at T_c . The magnitude of the ratio of the thermal resistance just above to that just below T_c is in fair quantitative agreement with that expected using the two-fluid model. Between 21.5 bar and the melting pressure the thermal resistance decreases much less rapidly as the temperature decreases through T_c , is history and heat-flow dependent, and may show critical-velocity effects. As T decreases through a lower temperature T_{AB} the resistance *decreases rapidly* and becomes history and heat-flow independent. At high enough pressures the "nonlinear" liquid may be supercooled through T_{AB} so that the linear-nonlinear transition is never observed.

These facts are depicted on a phase diagram in Fig. 1 using both the magnetic temperature scale T^* and an absolute scale T_{sound} based on zero-sound attenuation in normal liquid as described in earlier work.⁵ The region of extraordinary behavior in the liquid is bounded by a line of second-order transitions T_c and by the melting curve. It is divided into two parts, ³He-A and ³He-B, by the line of thermal-resistance discontinuities T_{AB} . Although we are unable to detect an entropy change at the AB transition, we nevertheless *suspect* for the following reasons that the T_{AB} line belongs on a phase diagram and may be a line of first-order transitions terminating at a "polycritical" point (PCP) on the T_c line. (1) It is possible²⁴ to supercool through T_{AB} . (2) The line T_{AB} extrapolates into the melting curve 0.5–0.6 mK below the temperature where the line T_c intersects the melting curve; this is the approximate displacement of the "B" feature from the "A" feature on the pressurization curve.^{11,12} (3) Where the line T_{AB} extrapolates into the line T_c , the slope dP_c/dT_c either changes rapidly or is discontinuous with $(dP_c/dT_c)_>/(dP_c/dT_c)_< \simeq 1.4$. Since T_{AB}^* and T_c^* are determined using differ-

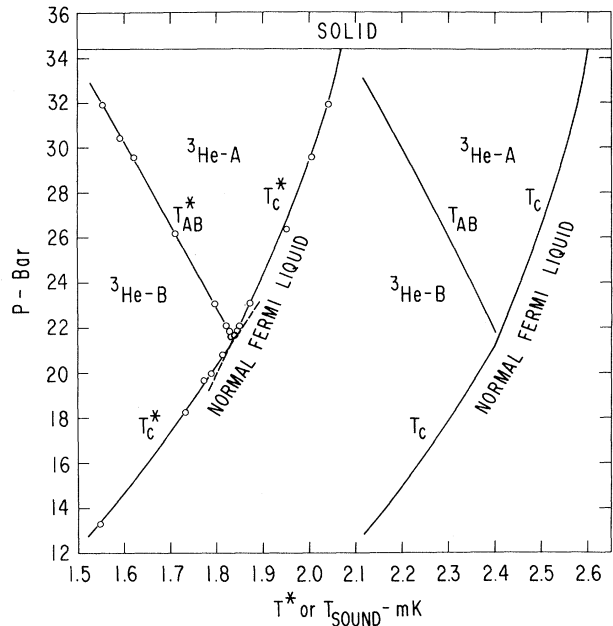


FIG. 1. Partial phase diagram of ³He in zero external magnetic field. Both measured magnetic temperatures T^* and tentative absolute temperatures T_{sound} (from Ref. 5) are shown.

ent criteria¹³ and both are somewhat uncertain, precise details of the phase diagram near the PCP at 21.5 bar and 2.4 mK cannot be given. Some features of the phase diagram were anticipated by Anderson and Brinkman.¹⁴

The demagnetization cell is shown schematically at the top of Fig. 2. The main refrigerant and lower thermometer T_1^* is 13.56 g of cerium magnesium nitrate (CMN) powder into which a hole 2 mm diam and 11 mm long has been drilled. The upper thermometer T_2^* is 10 mg CMN powder. The 2.0-mm-diam thermal-resistance column has a heater 18 mm above the main CMN. The externally applied heat-flow rate is \dot{Q}_e . We measured $T_2^* - T_1^*$ with \dot{Q}_e constant as the cell warmed under the residual heat leak, using different values of \dot{Q}_e on successive demagnetizations. Because of the different packing and shape of the thermometers, $T_2^* - T_1^*$ for $\dot{Q}_e = 0$ was about 0.34 mK over most of the temperature range. The temperature difference depended linearly on \dot{Q}_e above T_c^* and in the ³He-B region except very near T_c^* ; however, the response was complicated in ³He-A and at T_{AB}^* . In Fig. 2(a) typical measurements in ³He-B near T_c^* are shown. The important qualitative result is the *rise* in $T_2^* - T_1^*$ on warming near T_c^* . Even for $\dot{Q}_e = 0$ a rise is seen; this results from residual

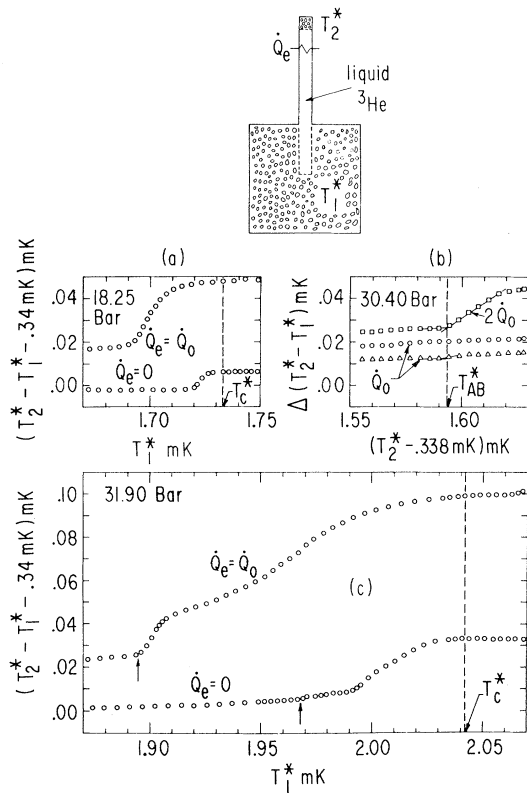


FIG. 2. Schematic cell diagram and typical examples of experimental data. $\dot{Q}_0 = 2.8 \times 10^{-3}$ erg/sec. In (b) the change in $T_2^* - T_1^*$ is shown rather than $T_2^* - T_1^*$ since this figure demonstrates both linearity and history dependence.

heat leak down the column. Thermal resistance starts to increase before T_2^* has reached T_c^* . This onset temperature depends on \dot{Q}_e . Typical results in $^3\text{He-A}$ near T_c^* are shown in Fig. 2(c) for the same values of \dot{Q}_e as above. Although the thermal transition T_c^* is not broadened, the resistive transition is broad, history dependent (not shown), and shows a reproducible onset-temperature feature (arrows). Typical dependence of $\Delta(T_2^* - T_1^*)$ on \dot{Q}_e near T_{AB}^* is shown in Fig. 2(b). The upper and lower curves show both the linear dependence of $\Delta(T_2^* - T_1^*)$ on \dot{Q}_e below T_{AB}^* and the \dot{Q}_e -dependent resistance which develops when T_2^* reaches T_{AB}^* . For points just to the right of T_{AB}^* , T_2^* is increasing rapidly with time; the ramp reflects transient, not steady-state, response. The middle curve corresponds to a higher than usual minimum temperature and shows no A-to-B transition, illustrating both supercooling and the history-dependent resistance of $^3\text{He-A}$.

Because of probable difficulties with the tem-

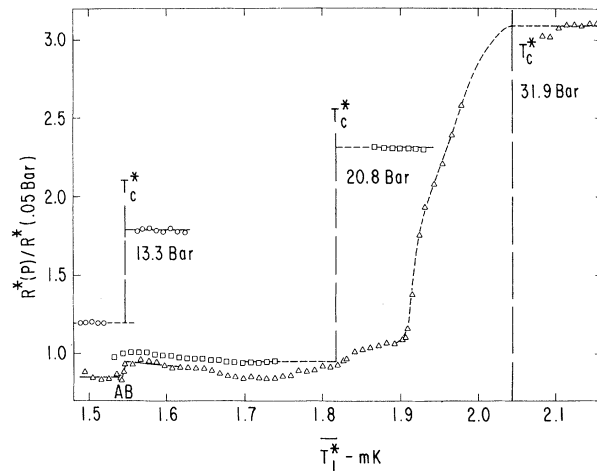


FIG. 3. Thermal resistances at three pressures reduced using the measured resistance at 0.05 bar. $\langle T_1^* \rangle$ is the average temperature in the column, referred to the lower thermometer. In the region near T_c^* there are two phases in the column.

perature scale, quantitative thermal resistance data at pressure P were reduced by dividing the measured resistance, $R^*(P) \equiv \Delta(T_2^* - T_1^*) / \Delta \dot{Q}_e$, by that measured at 0.05 bar. The latter is probably proportional to T in the present temperature range.¹⁵ The results for three pressures are shown in Fig. 3. No points are plotted in the transition region for 13.3 and 20.8 bar; the curve shown for 31.9 bar has $\dot{Q}_e = 2.8 \times 10^{-3}$ erg/sec, but R^* depends on \dot{Q} and history in the $^3\text{He-A}$ region. Several observations may be made on the R^* data. (1) To compare with theory^{9,10} using normal-state properties, we extrapolated $R^*(P)/R^*(0.05 \text{ bar})$ into T_c^* . Experimental values thus obtained for the ratio $(R_{>^*}/R_{<^*})_{\text{expt}}$ of the resistance just above to that just below T_c^* for $^3\text{He-B}$ are given in Table I. In the two-fluid model this ratio is $1 + (\kappa_h/\kappa_d)$, where κ_d and κ_h are the diffusive and hydrodynamic conductivities, respectively, at T_c .

TABLE I. Analysis of thermal-resistance data using a two-fluid model.

P (bar)	$R_{>^*}/R_{<^*}$		T_c (mK)
	Expt.	Calc.	
13.3	1.5	1.5	2.14
18.2	2.0	2.3	2.31
19.9	2.3	2.7	2.36
20.8	2.4	3.0	2.39
23.0	2.8 ^a	3.6	2.44
31.9		8.6	2.58

^a Extrapolated through $^3\text{He-A}$ phase.

One has

$$\frac{R_{>}^*}{R_{<}^*} = 1 + \frac{d^2}{32} \left[\frac{T_c (\gamma T_c)^2}{\eta \kappa_d} \right] = 1 + \frac{T_c^6 \gamma^2 d^2}{32 (\eta T^2) (\kappa_d T)}, \quad (1)$$

where γT is the normal-state entropy per unit volume, d is column diameter, and ηT^2 and $\kappa_d T$ are temperature-independent normal Fermi-liquid transport quantities.^{5,15} Inserting the approximately known values of these parameters into (1) we find the results labeled $(R_{>}^*/R_{<}^*)_{\text{calc}}$ in Table I. There is fair quantitative agreement, suggesting that a two-fluid model may be valid for ${}^3\text{He-B}$. An alternative model, assuming diffusive conductivity only with κ_d proportional to the specific heat, does not seem to fit the data. Values of $(R_{>}^*/R_{<}^*)_{\text{expt}}$ are subject to errors both in extrapolation to T_c and in a ${}^3\text{He}$ resistance within the main CMN, where heat flow will be diffusive only. The latter effect varies like κ_h/κ_d and is approximately 2% at the PCP; but for $T/T_c \approx 0.8$ and particularly at higher P (e.g., ${}^3\text{He-B}$ data at 31.9 bar), the effect may be as much as a factor of 2 and will help to improve agreement between experiment and theory. (2) The magnitude and temperature dependence of R^* in ${}^3\text{He-B}$ for the small temperature range of the measurements below T_c are curiously close to those for low-pressure ${}^3\text{He}$ where $\kappa_d T$ is constant. Assuming mainly hydrodynamic heat flow below T_c , where $\kappa_h \propto TS^2/\eta_n$ for entropy S and normal viscosity η_n , a resistance linear in T suggests that η_n has a temperature dependence like $(TS)^2$ and thus like $(T/T_c)^a$ with a in the range¹⁷ 7 to 10. (3) We draw no quantitative conclusions on subcritical thermal resistance of ${}^3\text{He-A}$ but note that for small \dot{Q} , Fig. 2(b), the change in R^* at the AB transition is small, indicating similar resistances.

The onset of increased resistance in ${}^3\text{He-A}$ at points such as those marked by arrows in Fig. 2(c) shows an approximately linear relation between the total \dot{Q} and the displacement between the onset temperature and T_c . This suggests, after some calculation and again in the context of a two-fluid model, a superfluid critical velocity of about 10^{-1} cm/sec.

Interpretation of the wire-damping experiments⁴ is also illuminated by the present observations.

(1) The rapid increase of damping as T increases near the $B \rightarrow A$ transition may reflect a transition from subcritical to critical flow.⁸ (2) The history-dependent damping in ${}^3\text{He-A}$ may represent critical flow conditions rather than thermal relaxation. (3) The damping probably cannot be

readily interpreted near "A" where the viscous penetration depth is large. However, both near the starting temperature in the liquid and in ${}^3\text{He-B}$, the amplitude may be approximately proportional to $(\rho_n \eta_n)^{-1/2}$, where ρ_n is normal-fluid density.¹⁶ Assuming that $\rho_n \propto T/T_c$ ¹⁷ and that $\eta_n \propto (T/T_c)^8$ just below T_c , we find that at temperatures somewhat below the $A-B$ transition the wire's vibration amplitude should be somewhat less than its value at 13 mK. This is in the range of the observations.

We gratefully acknowledge conversations with Dr. S. Putterman, Dr. J. C. Wheeler, Dr. J. M. Goodkind, Dr. D. M. Lee, and Dr. R. C. Richardson.

†Work supported by the U. S. Atomic Energy Commission under Contract No. AT(04-3)-34, P.A. 143.

*Alfred P. Sloan Research Fellow. Permanent address: Department of Physics, Massachusetts Institute of Technology, Cambridge, Mass. 02139.

¹R. A. Webb, T. J. Greytak, R. T. Johnson, and J. C. Wheatley, Phys. Rev. Lett. **30**, 210 (1973).

²D. D. Osheroff, W. J. Gully, R. C. Richardson, and D. M. Lee, Phys. Rev. Lett. **29**, 920 (1972).

³D. T. Lawson, W. J. Gully, S. Goldstein, R. C. Richardson, and D. M. Lee, Phys. Rev. Lett. **30**, 541 (1973).

⁴T. A. Alvesalo, Yu. D. Anufriyev, H. K. Collan, O. V. Lounasmaa, and P. Wennerström, Phys. Rev. Lett. **30**, 962 (1973).

⁵D. N. Paulson, R. T. Johnson, and J. C. Wheatley, Phys. Rev. Lett. **30**, 829 (1973), and unpublished.

⁶J. M. Dundon, D. L. Stolfa, and J. M. Goodkind, Phys. Rev. Lett. **30**, 843 (1973).

⁷D. F. Brewer and D. O. Edwards, Proc. Roy. Soc., Ser. A **251**, 247 (1959).

⁸D. F. Brewer and D. O. Edwards, Phil. Mag. **6**, 775 (1961).

⁹F. London and P. R. Zilsel, Phys. Rev. **74**, 1148 (1948).

¹⁰C. J. Gorter and J. H. Mellink, Physica (Utrecht) **15**, 285 (1949).

¹¹D. D. Osheroff, R. C. Richardson, and D. M. Lee, Phys. Rev. Lett. **28**, 885 (1972).

¹²R. T. Johnson, D. N. Paulson, C. B. Pierce, and J. C. Wheatley, Phys. Rev. Lett. **30**, 207 (1973).

¹³The thermal transitions T_c^* were determined as in Ref. 1.

¹⁴P. W. Anderson and W. F. Brinkman, Phys. Rev. Lett. **30**, 1108 (1973).

¹⁵W. R. Abel, R. T. Johnson, J. C. Wheatley, and W. Zimmermann, Jr., Phys. Rev. Lett. **18**, 737 (1967), and further measurements in the present experiments.

¹⁶M. A. Black, H. E. Hall, and K. Thompson, J. Phys. C: Proc. Phys. Soc., London **4**, 129 (1971).

¹⁷P. G. de Gennes, *Superconductivity of Metals and Alloys* (Benjamin, New York, 1966), p. 172; A. J. Leggett, Phys. Rev. **140**, A1869 (1965).